Biogeosciences Discuss., 12, 3419–3468, 2015
www.biogeosciences-discuss.net/12/3419/2015/
doi:10.5194/bgd-12-3419-2015

Biogeosciences
Discussions
Open Access

Eddy covariance methane flux measurements over a grazed pasture: effect of cows as moving point sources

R. Felber[1,2], **A. Münger**[3], **A. Neftel**[1], **and C. Ammann**[1]

[1]Agroscope Research Station, Climate and Air Pollution, Zurich, Switzerland
[2]ETH Zurich, Institute for Animal Sciences, Zurich, Switzerland
[3]Agroscope Research Station, Milk and Meat Production, Posieux, Switzerland

Received: 21 January 2015 – Accepted: 17 February 2015 – Published: 24 February 2015

Correspondence to: R. Felber (raphael.felber@agroscope.admin.ch)

Published by Copernicus Publications on behalf of the European Geosciences Union.

Abstract

Methane (CH_4) from ruminants contributes one third to global agricultural greenhouse gas emissions. Eddy covariance (EC) technique has been extensively used at various flux sites to investigate carbon dioxide exchange of ecosystems. Since the development of fast CH_4 analysers the instrumentation at many flux sites have been amended for these gases. However the application of EC over pastures is challenging due to the spatial and temporal uneven distribution of CH_4 point sources induced by the grazing animals. We applied EC measurements during one grazing season over a pasture with 20 dairy cows (mean milk yield: 22.7 $kg\,d^{-1}$) managed in a rotational grazing system. Individual cow positions were recorded by GPS trackers to attribute fluxes to animal emissions using a footprint model. Methane fluxes with cows in the footprint were up to two orders of magnitude higher than ecosystem fluxes without cows. Mean cow emissions of $423 \pm 24\,g\,CH_4\,head^{-1}\,d^{-1}$ (best guess of this study) correspond well to animal respiration chamber measurements reported in the literature. However a systematic effect of the distance between source and EC tower on cow emissions was found which is attributed to the analytical footprint model used. We show that the EC method allows to determine CH_4 emissions of grazing cows if the data evaluation is adjusted for this purpose and if some cow distribution information is available.

1 Introduction

Methane (CH_4) is after carbon dioxide (CO_2) the second most important human induced greenhouse gas (GHG) and contributes about 17 % to the global anthropogenic radiative forcing (Myhre et al., 2013). Agriculture is estimated to contribute about 50 % of total anthropogenic emissions of CH_4 while enteric fermentation of livestock alone accounts for about one third (Smith et al., 2007). For Switzerland these numbers are even higher, with 85 % total agricultural contribution and 67 % from enteric fermentation alone, but still afflicted with considerable uncertainty (Hiller et al., 2014). Measurements

BGD
12, 3419–3468, 2015

of these emissions are therefore important for national GHG inventories and to assess the effect on global scale.

Direct measurements of enteric CH_4 emissions are commonly made on individual animals using open-circuit respiration chambers (Münger and Kreuzer, 2006, 2008) or the SF_6 tracer technique (Lassey, 2007; Pinares-Patiño et al., 2007). Both methods are labor-intensive and thus are usually applied only for rather short time intervals (several days). Although the respiration chamber method needs a costly infrastructure and investigates animals in a constrained situation, it presently is the reference technique to estimate animal breed and diet related differences in CH_4 emissions.

Recently also micrometeorological measurement techniques have been tested to estimate ruminant CH_4 emissions on the plot scale and compare animal scale emissions to field scale emissions. These approaches are based on average concentration measurements: backward Lagrangian stochastic dispersion, mass balance for entire paddocks, and gradient methods (Harper et al., 1999; Laubach et al., 2008; Leuning et al., 1999; McGinn et al., 2011). They have in common that they integrate over a group of animals and are usually applied over specifically designed relatively small fenced plots.

Among the micrometeorological methods, the eddy covariance (EC) approach is considered as the most direct to measure the trace gas exchange of ecosystems (Dabberdt et al., 1993), and it is used as standard method for CO_2 flux monitoring in regional and global networks (e.g. Aubinet et al., 2000; Baldocchi, 2003). Advances in the commercial availability of tunable diode laser spectrometers (Peltola et al., 2013) that measure CH_4 (and N_2O) concentrations at sampling rates of 10 to 20 Hz have steadily increased the number of ecosystem monitoring sites also measuring the exchange of these GHG. However the number of studies made over grazed pastures is still low although such measurements are of importance to assess the full agricultural GHG budget. Baldocchi et al. (2012) showed the challenge of measuring CH_4 fluxes affected by cattle and stressed the importance of position information of these point sources. Dengel et al. (2011) used EC measurements of CH_4 fluxes over a pasture

BGD
12, 3419–3468, 2015

with sheep. But the interpretation of the fluxes had to be based on rough assumptions because the distribution of animals on the (large) pasture was not known.

An ideal requirement for micrometeorological measurements is a spatially homogeneous source area around the measurement tower (Munger et al., 2012), which is often hard to achieve in reality. Although EC fluxes are supposed to average over a certain upwind "footprint" area (Kormann and Meixner, 2001), the effect of stronger inhomogeneity in the flux footprint (FP), like ruminating animals contributing to the CH_4 flux, have not been studied in detail. These animals are not always on the pasture (away for milking) and move around during grazing. They are in changing numbers up- or downwind of the measurement tower and represent non-uniformly distributed point sources. In addition cows are relatively large obstacles and may distort the wind and turbulence field making the application of EC measurement disputable.

The main goal of the present study was to test the applicability of EC measurement for in-situ CH_4 emission measurements over a pasture with a dairy cow herd under realistic grazing situations. GPS position data of the individual cows were recorded to know the distribution of the animals and to distinguish contributions of direct animal CH_4 release (enteric fermentation) and of CH_4 exchange at the soil surface to measured fluxes. Cow attributed fluxes were converted to animal related emissions using a flux FP model in order to test the EC method in comparison to literature data. Additionally the following questions were addressed in the study:

- Are animal emissions derived from EC fluxes consistent and independent of the distance of the source?
- Is a compensation for the heterogeneous distribution of the cows by footprint calculations reliable?
- How detailed has the position information to be? Is the position of each cow needed? Do footprint corrected emissions based on paddock area reveal comparable results?

BGD
12, 3419–3468, 2015

– Do cows influence the aerodynamic roughness length used by footprint models? To what extend is the footprint weight influenced by the presence of the cows?

2 Material and methods

2.1 Study site and grazing management

The experiment was conducted on a pasture at the Agroscope research farm near Posieux on the Swiss western plateau (46°46′04″ N 7°06′28″ E). The research farm is located at an altitude of 642 m above sea level with a long-term (1981–2010) annual rain amount of 1075 mm and temperature of 8.9 °C (MeteoSchweiz, 2014). The average temperature in 2013 was 8.6 °C. During the grazing period the average temperature was 14.3 °C ranging from 3.6 to 30.9 °C (hourly values). The temperatures in March and May were 2.8 and 2.9 °C below the long-term average. In the summer months temperatures were close to the long-term average but rainfall was considerably reduced (35 % of the long-term average in June and 75 % in July). The total amount of rain in this year of 1031 mm was comparable to the long-term average. The pasture vegetation consists of a 85/15 % grass-clover mixture (mainly *Lolium perenne* and *Trifolium repens*). It was last renovated in August 2007 and has since then been used as pasture for various livestock (dairy, beef cattle, calves). On average the pasture was fertilized with 120 kg nitrogen (N) per year in addition to the livestock excreta. In 2013, 70 $kg\,N\,ha^{-1}$ were applied in form of cattle slurry before the start of the experiment and 50 $kg\,N\,ha^{-1}$ as urea in June. The soil is classified as stagnic Anthrosol with a loam texture. The vegetation growth was retarded at the beginning of the grazing season due to the colder spring and the wetter conditions during April and May. The dry summer (June and July) also led to shortage of fodder on the paddocks. Therefore additional pasture areas, which were not covered by the EC measurement, were needed to feed the animals.

BGD
12, 3419–3468, 2015

The staff and facilities at the research farm provided the herd management and automated individual measurements of milk yield and body weight at each milking. Milk was sampled individually on one day per week and analyzed for main components. Monthly energy-corrected milk (ECM) yield of the cows was calculated from daily milk yield and the contents of fat, protein and lactose (Arrigo et al., 1999). Monthly ECM yield decreased over the first three months but overall was fairly constant in time with a mean value of 22.7 ± 5.5 (SD) kg. The average live weight of 640 ± 70 (SD) kg slightly increased by around 6 % over the grazing season.

The field (3.6 ha) was divided into six equal paddocks (PAD1 to PAD6) of 0.6 ha each (Fig. 1). The arrangement of the paddocks was chosen to create situations with the herd grazing in differing distances to the EC tower. The present study covers one full grazing season 9 April–4 November 2013. 20 dairy cows were managed in a rotational grazing system during day and night. Depending on initial herbage height the cows typically grazed for 1 to 2 days on a paddock. The herd consisted of Holstein and Red Holstein x Simmental crossbred dairy cows and was managed with an objective to keep the productivity of the herd relatively constant in time. For this reason individual cows drying off were replace with animals in full production on the following dates: 12 June (1 cow), 17 July (6), 28 August (3), and 11 September (3). Also for herd management reasons the number of cows was slightly reduced at the beginning (17 cows until 24 April) and at the end of the experiment (18 cows from 10 October on). The cows left the pasture twice a day for milking in the barn where they were also offered concentrate supplement (usually < 10 % of total diet dry matter) according to their milk production level. The paddock leaving time was around 4 a.m. and 3 p.m. but varied slightly depending on workload in the barn and air temperature. If there was risk of frost, the cows stayed in the barn overnight (58 nights), and if the daytime air temperature exceeded about 28 °C before noon, the cows were moved into the barn for shade (19 days). Waterlogged soil condition entirely prohibited grazing on the pasture between 12 and 13 April. In total the cows were grazing on the study field for 198

BGD
12, 3419–3468, 2015

Title Page
Abstract | Introduction
Conclusions | References
Tables | Figures
◄| |►
◄ ►
Back | Close
Full Screen / Esc
Printer-friendly Version
Interactive Discussion

half-days and for another 157 half-days on nearby pastures not measured by the EC tower.

2.2 Eddy covariance measurements

2.2.1 Instruments and set up

The EC measurement tower was placed in the middle of the pasture and was enclosed by a 2-wire electric fence to avoid animal interaction with the instruments (Fig. 1). The 3-D wind vector components u, v (horizontal) and w (vertical), as well as temperature were measured by an ultra-sonic anemometer (Solent HS-50, Gill Instruments Ltd., UK) mounted on a horizontal arm on the tower, 2 m above ground level. Methane, CO_2, and water vapor concentrations were measured by cavity-enhanced laser absorption technique (Baer et al., 2002) by a fast greenhouse gas analyzer (FGGA; Los Gatos Research Inc., US). The FGGA was placed in a temperature-conditioned trailer in 20 m distance (NNE) from the EC tower and was operated in high flow mode at 10 Hz. A vacuum pump (XDS35i Scroll Pump, Edwards Ltd., UK) pulled the sample air through a 30 m long PVC tube (8 mm ID) and through the analyzer at a flow rate of about 45 $\mathrm{sL\,min^{-1}}$. The inlet of the tube was placed slightly below the center of the sonic anemometer head at a horizontal distance of 20 cm. Two particle filters with liquid water traps (AF30 and AFM30, SMC Corp., JP) were included in the sample line. The 5 µm air-filter (AF30), installed 1 m away from the inlet, avoided contamination of the tube walls. The micro air-filter (AFM30; 0.3 µm) was installed at the analyzer inlet.

The noise level of the FGGA for fast CH_4 concentration measurements depended on the cleanness of the cavity mirrors. It was determined as minimum of the SD of the 10 Hz data. At the beginning the noise levels was at 15 ppb but gradually increased to 38 ppb over time due to progressive contamination. In July 2013 the noise abruptly increased without any explanation but the cleaning had to be postponed until mid of August. During this period the noise level was 230 to 400 ppb. After the cleaning the noise was even lower (around 7 ppb) than at the beginning.

BGD
12, 3419–3468, 2015

The gas analyzer was calibrated at intervals of approximately two months with two certified standard gas mixtures (1.5 ppm CH_4/350 ppm CO_2 and 2 ppm CH_4/500 ppm CO_2; Messer Schweiz AG, CH). An excess of the standard gas was bi-passed by a T-fitting to the device which was set into low measurement mode at 1 Hz using the internal pump. The calibration showed that the accuracy did not vary over time, except for the period when the measurement cell was very strongly contaminated.

The data streams of the sonic anemometer and the dry air mixing ratios from the FGGA instrument were synchronized in real-time by a customized LabView (LabView 2009, National Instruments, US) program and stored as raw data in daily files for offline analysis.

Standard weather parameters were measured by a customized automated weather station (Campbell Scientific Ltd., UK).

2.2.2 Flux calculation

Fluxes were calculated for 30 min intervals by a customized program in the R software (R Core Team, 2014). First, each raw 10 Hz time series was filtered for values outside the physically plausible range ("hard flags") and the sonic data (wind and temperature) were subject to a de-spiking ("soft flags") routine according to Schmid et al. (2000); replacing values that exceed 3.5 times the SD within a running time window of 50 s. Filtered values were counted and replaced by a running mean over 500 data points. No de-spiking was applied for CH_4 because a potentially large effect on resulting fluxes was found as illustrated in Fig. 2. With cows in the FP the CH_4 concentration showed many large peaks (Fig. 2a), whereas for situations without cows the variability range was much lower (Fig. 2b). If the de-spiking routine is applied to the time series, this has a strong effect in the case with cows in the FP. 454 data points are replaced in this 30 min interval and the remaining concentration data are limited to 3500 ppb. The corresponding flux is reduced from 1322 to 981 nmol m^{-2} s^{-1} (−26 %). The time series not influenced by cows shows no distinct spikes and only 5 data points are removed by the de-spiking routine without significant effect on the resulting flux. Prior to the covariance calculation the wind components were rotated by the double rotation method (Kaimal and Finnigan, 1994) to align the wind coordinate system into the mean wind direction, and the scalar variables were linearly detrended.

The EC flux is defined as the covariance between the vertical wind speed and the trace gas mixing ratio (Foken et al., 2012a). Due to the tube sampling of the FGGA instrument there is a lag time between the recording of the two quantities. Therefore, the CH_4 flux was determined in a three-stage procedure: (i) for all 30 min intervals the maximum absolute value (positive or negative) of the cross-covariance function and its lag position ("dynamic lag") was searched within a lag time window of ±50 s. (ii) The "fixed lag" was determined as the mode (most frequent value) of observed dynamic lags over several days allowing for longer-term temporal changes due to the FGGA operational conditions. (iii) For the final data set, the flux at the fixed lag was taken, if the deviation between the dynamic and the fixed lag was larger than 0.36 s, else the flux at the dynamic lag was taken. The fixed lag for the CH_4 flux in this study was around 2 s.

For large emission fluxes with cows in the FP a pronounced and well determined peak in the cross-covariance function could be found close to the expected lag time (Fig. 3a). For small fluxes the peak can be hidden in the random-like noise of the cross-covariance function and the maximum value may be found at an unplausible dynamic lag position (Fig. 3b). In this case the flux at the fixed lag is statistically more representative.

The air transportation through the long inlet tube (30 m) and the filters led to high-frequency loss in the signal (Foken et al., 2012b). To determine the damping factor sufficient flux intervals with good conditions are needed, i.e., flux intervals with large fluxes. CO_2 exchange over grasslands typically reveals significant fluxes well above the detection limit, whereas the CH_4 fluxes are much smaller and often around the flux detection limit. Because both quantities were measured by the same device, we assumed that CH_4 fluxes had the same high-frequency loss as determined for the

BGD
12, 3419–3468, 2015

more significant CO_2 fluxes. High-frequency loss was calculated by the "ogive"-method as described in Ammann et al. (2006). In short, the damping factor was calculated by fitting the normalized cumulative co-spectrum of the trace gas flux to the normalized sensible heat flux co-spectrum at the cut-off frequency of 0.065 Hz. The minor high-frequency damping of the sensible heat flux itself was calculated according to (Moore, 1986). A total damping of 10 to 30 % depending mainly on wind speed was found for the presented setup, and the fluxes were corrected for this effect.

The mixing ratios measured by the FGGA were internally corrected for the amount of water vapor (at 10 Hz) and stored as "dry air" values. Since also temperature fluctuations are supposed to be fully damped by the turbulent flow (Reynold number = 10 000) in the long inlet line, no further correction for correlated water vapor and temperature fluctuations (WPL density correction, Webb et al., 1980) had to be applied.

2.2.3 Detection limit and flux quality selection

The flux detection limit was determined by analyzing the cross-covariance function of fluxes dominated by general noise, i.e., fixed lag cases without significant covariance peak. Additionally, the selection was limited to smaller fluxes (range around zero for which more fixed lag than dynamic lag cases were found: here ±26 nmol m^{-2} s^{-1}) in order to exclude cases with unusually high non-stationarity effects. The uncertainty of the noise dominated fluxes was determined from variability (SD) of two 50 s windows on the left and the right side of the covariance function (Fig. 3). The detection limit was determined as 3 times the average of these SDs.

All measured EC fluxes were selected using basic quality criteria. The applied limits were chosen based on theoretical principles and statistical distributions of the tested quantities. Only cases which fulfilled the following criteria were used for calculations:

- less than 10 hard flags in wind and concentration time series
- vertical vector rotation angle (tilt angle) in plausible range between −2 and +6°

- wind direction within sectors 25 to 135° and 195 to 265° to exclude cases that are affected by the farm facilities in the north and in the south of the study field (by non-negligible flux contribution, non-stationary advection, distortion of wind field and turbulence structure).

- fluxes above the detection limit need a significant covariance peak (dynamic lag determination)

Moving sources in the FP lead to strong flux variations which are normally identified by the stationarity criterion (Foken et al., 2012b). We did not apply a stationarity test, because it removed up to 5 % of cases with cow contributions. Table 1 shows the reduction in number of fluxes due to the quality selection criteria.

2.3 GPS method for deriving animal CH_4 emission

To assess the reliability of EC flux measurements of CH_4 emissions by grazing cows, the measured fluxes (F_{EC}) had to be converted to average cow emissions (E) per animal and time. This was done using three different information levels about animal position and distribution on the pasture:

1. GPS method: use of time-resolved position for each animal from GPS cow sensors (this section)

2. PAD method: use of detailed paddock grazing time schedule (Sect. 2.4)

3. FIELD method: using only the seasonal average stocking rate on the measurement field without grazing schedule details (Sect. 2.5).

For the GPS and PAD method, the selection of fluxes was further restricted (Table 1) by discarding situations when cows were moved from/to pasture. Additionally fluxes leading to emission outliers were removed by applying the boxplot function of R (R Core Team, 2014). 257 (2.5 %) and 271 (2.7 %) fluxes remained for the calculation of

BGD
12, 3419–3468, 2015

cow emissions using the GPS and PAD method, respectively. For the FIELD method 3630 (36 %) fluxes were used.

2.3.1 Animal position tracking

For the animal position tracking each cow was equipped with a commercial hiking GPS device (BT-Q1000XT, Qstarz Ltd., TW). The GPS loggers using the WAAS, EGNOS and MSAS correction (Witte and Wilson, 2005) continuously recorded the position at a rate of 0.2 Hz. Each GPS device was connected to a modified battery pack with 3 V × 3.6 V lithium batteries to extend the battery lifetime up to 10 days. GPS data was collected from the cow sensors weekly during milking time, and at the same occasion also the batteries were exchanged. GPS coordinates were transformed from World Geodetic System (WGS84) to the metric Swiss national grid (CH1903 LV95) coordination system. GPS data was filtered for cases with low quality depending on satellite constellation (positional dilution of precision PDOP ≤ 5). Each track was visually inspected for malfunction to exclude additional bad data not excluded by the PDOP criterion. Smaller gaps (< 1 min) in the GPS data of individual cow tracks were linearly interpolated. The total coverage of available GPS data was used as quality indicator for each 30 min interval. The position data were used to distinguish between 30 min intervals when the cows were on the study field or elsewhere (barn or other pasture), or moved between the barn and the pasture.

The accuracy of the GPS devices was assessed by a fixed point test with six devices placed directly side by side for five days. Each device showed an individual variability in time (Fig. 4) and some systematic deviation from the overall mean position (determined from very good data with PDOP < 2 of all devices). The accuracy of each device was calculated as the 95 % quantile of deviations. It ranged from 1.9 to 4.3 m for the six devices. We assessed an accuracy of 4.5 m as sufficient for EC measurements, since the accuracy of the EC footprint for a 30 min interval lies in the same order of magnitude. The GPS data coverage was good for continuously operating sensors attached to animals. In 92 % of the cases when cow fluxes could be measured more than 70 %

BGD
12, 3419–3468, 2015

of all GPS devices delivered usable data, which was considered as sufficient for the quantification of cow FP contribution.

2.3.2 Footprint calculations

An EC flux measurement represents a weighted spatial average over a certain upwind surface area called flux FP. The FP weighting function can be estimated by dispersion models. Kormann and Meixner (2001) published a FP model (KM01) based on an analytical solution of the advection-dispersion equation using power-functions to describe the vertical profiles. The basic Eq. (1) describes the weight function φ of the relative contribution of each upwind location to the observed flux with the x coordinate for longitudinal and y coordinate for lateral distance.

$$\varphi(x,y) = \frac{1}{\sqrt{2\pi}\cdot D\cdot x^E} e^{\frac{-y^2}{2\left(D\cdot x^E\right)^2}} \cdot C\cdot x^{-A}\cdot e^{\frac{-B}{x}} \tag{1}$$

The terms A to E are functions of the necessary micrometeorological input parameters ($z-d$: aerodynamic height of the flux measurement; u_*: friction velocity; L: Monin–Obukhov length; σ_v: SD of the lateral wind component; wd: wind direction; $\overline{u}$: mean wind speed) which were all measured by the EC system.

The FP weight function also needs the aerodynamic roughness length (z_0) as input parameter. It can be calculated as described in Neftel et al. (2008) from the other input parameters $z-d$, u_*, L, and $\overline{u}$ by solving the following wind-profile relationship:

$$\overline{u}(z-d) = \frac{u_*}{k}\left[\ln\left(\frac{z-d}{z_0}\right) - \psi_H\left(\frac{z-d}{L}\right)\right] \tag{2}$$

However, the determination of z by this equation is sensitive to the quality of the other parameters and especially problematic in low-wind conditions with relatively high uncertainty in the measured u_*. Because z_0 is considered approximately constant for given grass canopy conditions, its average seasonal course for the measurement field

BGD
12, 3419–3468, 2015

Eddy covariance methane flux measurements over a grazed pasture

R. Felber et al.

was parameterized by fitting a polynomial to individual results of Eq. (2) which fulfilled the following criteria: $\overline{u} > 1.5\,\mathrm{m\,s^{-1}}$ (see e.g., Graf et al., 2014), days without snow cover, and mean wind direction in the undisturbed sectors 25 to 135° and 195 to 265° (other wind direction showed relatively large variation of z_0).

Because of short-term variability in the vegetation cover and because of the potential impact of cows on z_0, a range of factor 3 to both sides of the fitted parameterization (see Fig. 8) was defined. If the individual 30 min z_0 value (derived by Eq. 2) was within this range it was directly used for the FP calculation. If z_0 exceeded this range it was restricted to the upper/lower bound of the range.

Assuming that each cow represents a (moving) point source of CH_4, the FP contribution of each 5 s-cow-position (Fig. 5a) was calculated according to Eq. (1). For each 30 min interval the average FP weight of the cow herd ($\overline{\varphi}_{\mathrm{cow}}$) was calculated as:

$$\overline{\varphi}_{\mathrm{cow}} = \frac{1}{n_{\mathrm{cow}} \cdot N} \sum_{k=1}^{n_{\mathrm{cow}}} \sum_{i=1}^{N} \varphi\left(x_{i,k}, y_{i,k}\right) \tag{3}$$

with n_{cow} denoting the number of cows in the herd, and N the number of available GPS data points per cow. To account for the uncertainty of the GPS position, each data point was blurred by adding 4 m in each direction from the original point. $\varphi(x_i, y_i)$ was calculated as the mean of the five $\varphi(x, y)$. $\overline{\varphi}_{\mathrm{cow}}$ values were accepted only for 30 min intervals where > 70 % of the GPS data was available and the input parameters L, u_*, and σ_v were of sufficient quality.

2.3.3 Calculation of average cow emission

The measured flux (F_{EC}) cannot be entirely attributed to the contribution of direct cow emissions within the FP. It also includes the CH_4 exchange flux of the pasture soil (including the excreta patches). This contribution is denoted as "soil flux" (F_{soil}) in the following. F_{soil} had to be quantified by selecting fluxes with no or negligible influence of cows based on the GPS FP evaluation and other selection criteria (Table 1).

BGD
12, 3419–3468, 2015

The GPS data allows the calculation of emissions based on actual observed cow distribution and the use of the average cow FP weights (Eq. 3). The average emission per cow for a 30 min interval is determined as:

$$E_{\text{cow}} = \frac{(F_{\text{EC}} - F_{\text{soil}})}{\overline{\varphi}_{\text{cow}}} \cdot \frac{1}{n_{\text{cow}}} \tag{4}$$

with n_{cow} denoting the number of cows and $\overline{\varphi}_{\text{cow}}$ the mean herd FP weight.

2.4 PAD method for deriving animal CH_4 emission

To assess the effect of the precision of cow position information on the determination of the average cow emission, an option with less detailed but easier to obtain position information was also applied and compared to the GPS approach. In the PAD method, no individual cow position information is used, but it is assumed, that the animal CH_4 source is evenly distributed over the actual grazing paddock area. For this approach, an accurate paddock grazing time schedule is needed.

2.4.1 Footprint calculation for paddocks

Neftel et al. (2008) developed a FP tool based on Eq. (1) that calculates the FP weights of quadrangular areas upwind of an EC tower. The source code was adapted and transferred to an R-routine in order to allow more complex polygons instead of quadrangles for the different sub-areas of interest (here paddocks).

Under the assumption that an observed flux originates from a known source and that the source is uniformly distributed over a defined paddock area, the measured fluxes can be corrected with the integrated FP weight (Neftel et al., 2008):

$$\Phi_{\text{PAD}} = \iint\limits_{\text{PAD area}} \varphi(x,y)\,\mathrm{d}x\mathrm{d}y \tag{5}$$

Discussion Paper | Discussion Paper | Discussion Paper | Discussion Paper |

BGD

12, 3419–3468, 2015

Eddy covariance methane flux measurements over a grazed pasture

R. Felber et al.

In the FP tool the domain which covers 99 % of the FP is divided into a grid of 200 (along-wind) times 100 (crosswind) cells, and for each cell the FP weight is calculated. The sum over all cells lying in the area of interest is the FP weight of the area (Eq. 5 and Fig. 5b). The FP model was already validated in a field experiment with a grid of artificial CH_4 sources and two EC flux systems (Tuzson et al., 2010).

2.4.2 Determination of average cow emission

With the information on grazing time and occupied paddock number, average cow emission for each 30 min interval is calculated as:

$$E_{\mathrm{cow}} = \frac{(F_{\mathrm{EC}} - F_{\mathrm{soil}}) \cdot A_{\mathrm{PAD}}}{\Phi_{\mathrm{PAD}}} \cdot \frac{1}{n_{\mathrm{cow}}} \tag{6}$$

with n_{cow} denoting the number of cows in the occupied paddock, A_{PAD} the area and Φ_{PAD} the FP fraction of the corresponding paddock. Emissions are calculated only for 30 min intervals where the cows were on the pasture, the FP weight of the grazed paddock Φ_{PAD} exceeds 0.1, and FP input parameters are of sufficient quality.

2.4.3 FIELD method for deriving animal CH_4 emission without position information

EC measurements are frequently performed over pastures, but usually no detailed information on the position and exact number of grazing animals and specific grazing times are available. If at least the average stocking rate over the grazing period is available and under the assumption that the cows are uniformly distributed over the entire pasture the time averaged cow emission can be calculated as:

$$\langle E_{\mathrm{cow}} \rangle = \left(\langle F_{\mathrm{EC}} \rangle - \langle F_{\mathrm{soil}} \rangle \right) \cdot A_{\mathrm{field}} \cdot \frac{1}{\langle n_{\mathrm{cow}} \rangle} \tag{7}$$

with $\langle F_{\mathrm{EC}} \rangle$ denoting the mean observed CH_4 flux of the grazing period, A_{field} the total pasture area, and $\langle n_{\mathrm{cow}} \rangle$ the mean number of cows on the study field over the grazing

BGD
12, 3419–3468, 2015

season. $\langle n_{cow} \rangle = 6.6$ heads is calculated as the total number of cows of each 30 min interval with cows on the study field plus 1/2 of the number of cows when the cows were moved between barn and pasture divided by the total number of 30 min intervals of the grazing period. For comparison reasons, the cow flux is calculated by subtraction of the average soil flux. This is of course only possible because the GPS data was available.

3 Results

3.1 Methane fluxes with and without cows

Observed 30 min CH_4 fluxes varied between −150 and 2801 $\mathrm{nmol\,m^{-2}\,s^{-1}}$ during the grazing season. Situation with cows close to the sensor revealed strong fluxes (Fig. 6b and c). For situations with no cows in the FP (Fig. 6a) or with cows further away measured fluxes were very small. For the cow emission calculations with FP consideration, fluxes were divided into situations with *near cows* (when grazing in PAD2 or PAD5 Fig. 6 white paddocks) and *far cows* (when grazing in one of the other paddocks PAD1, PAD3, PAD4, and PAD6 Fig. 6 gray paddocks).

For a systematic assessment of the relation between CH_4 flux and cow position and for the separation of cases representing pure soil fluxes, all quality selected fluxes were plotted against $\overline{\varphi}_{cow}$ in Fig. 7. It shows a clear relationship with a strong increase of fluxes only in the highest $\overline{\varphi}_{cow}$ range. Situations with *near cows* led to generally higher FP weights and fluxes than for the *far cows* situations. Based on Fig. 7, the limit $\varphi_{crit,\,cow} = 10^{-5}\,\mathrm{m^{-2}}$ was determined as the cut off for cow affected fluxes to be used for the calculation of E_{cow}. Cases with $\overline{\varphi}_{cow}$ below $\varphi_{crit,\,soil} = 10^{-7}\,\mathrm{m^{-2}}$ were classified as soil fluxes.

The soil flux values were found to be generally small but mostly positive in sign (typically in the range 0 to 15 $\mathrm{nmol\,m^{-2}\,s^{-1}}$ Fig. 7) indicating a continuous small emission by the soil and surface processes. The accuracy of these fluxes was difficult to quan-

BGD
12, 3419–3468, 2015

tify because they mostly had no well-defined peak in the covariance function and thus 92 % had to be calculated at the fixed lag. Even though temporal variations in median diurnal and seasonal cycles were observed (in the range of 1 to 7 $\mathrm{nmol\,m^{-2}\,s^{-1}}$), it was unclear whether these can be attributed to effects of environmental drivers or whether they result from non-ideal statistics and selection procedures. Also varying small contributions from cows on neighboring upwind fields could not be excluded. Therefore we used a conservative overall average estimate for the soil flux of $4 \pm 3\,\mathrm{nmol\,m^{-2}\,s^{-1}}$ with the uncertainty range of ±50 % covering the temporal variation of medians indicated above.

3.2 Footprints and cow influence

3.2.1 Roughness length

The 30 min values of the roughness length z_0 determined for wind speeds > 1.5 $\mathrm{m\,s^{-1}}$ showed a systematic variation over the year peaking in summer (Fig. 8) when the vegetation height ranged between 5 and 15 cm. Bi-weekly medians for situations with no cows in the FP ranged from 0.16 to 1.6 cm and corresponded well to the parameterized z_0. Cows in the FP (withers height *c*. 150 cm) slightly influenced z_0. The effect was distance dependent (Fig. 9). For cases with high FP weights of the cows (i.e., cows closer to the EC tower), z_0 was systematically up to 2 cm higher than the average parameterized z_0. However there was still a considerable scatter of individual values and variation with time. The range limits for z_0 (gray range in Fig. 8) were necessary to filter unplausible individual values under low wind or otherwise disturbed conditions. However, they were sufficiently large to include most of the cases influenced by cows. While for soil fluxes not influenced by cows 16 % (5 % below/11 % above) of the calculated z_0 values lay outside the accepted z_0-range, the respective portion was only slightly higher (2 % below/18 % above) for situations with cows in the FP.

BGD
12, 3419–3468, 2015

3.2.2 Footprint weights of cows and paddocks

Average cow FP weights (Eq. 3) ranged up to 2.9×10^{-4} and $0.7 \times 10^{-4}\,m^{-2}$ for the *near* and *far cows* situations (Fig. 10a). On the lower end they were limited by the cut-off value $\varphi_{crit,\,cow}$. The distribution of the *near cows* cases showed a pronounced right tail whereas the *far cows* cases were more left skewed. Figure 10b shows the FP fraction of the paddock in which the cows were grazing and which were used to calculate the emissions with the PAD method (Eq. 6). FP fractions for *far cows* were always lower than 25 % of the total FP area. For the majority of the *near cows* cases the contribution to the measured flux was more than 40 %.

3.3 Methane emission per cow

3.3.1 Overall statistics

The discrimination of fluxes into the classes *near* and *far cows* resulted in 194 and 63 30 min GPS based cow emission values, respectively. Using the PAD method, the corresponding numbers were only slightly higher (Table 1). Table 2 shows the estimated cow emissions for the three emission calculation schemes and for the two distance classes (*near cows*, *far cows*) if applicable. Emissions calculated for the *near cows* cases were significantly larger than emissions calculated for the *far cows* cases. The uncertainty of the mean (2× SE, calculated according to Gaussian error propagation) was lowest for the *near cows* of the GPS method. Emission results calculated with the PAD method were comparable to those of the GPS method considering the distance classes. The difference between median and mean values for GPS and PAD method were relatively small indicating symmetric distribution of individual values. Because the result of the FIELD method was calculated as temporal mean over the entire grazing period (with many small soil fluxes and few large cow influenced fluxes, see Fig. 7), the uncertainty could not be quantified from the variability of the individual 30 min data. Therefore we applied the FIELD method also to monthly periods and estimated the uncertainty ($\pm184\,g\,CH_4\,head^{-1}\,d^{-1}$) from those results ($n = 7$). It is much larger than for the two other methods and there exists also a considerable difference between the two different mean values.

3.3.2 Diurnal variations

Average diurnal cycle analysis for the *near cows* cases (Fig. 11) showed persistent CH_4 emission by the cows over the entire course of the day. For four hours of the day less than five values per hour were found, mainly around the two milking periods or during nighttime. Mean emissions per hour ranged from 288 to $560\,g\,CH_4\,head^{-1}\,d^{-1}$ with highest values in the evening and lowest in the late morning (disregarding hours with $n < 5$). Although the two grazing periods (evening/night: 5 p.m. to 3 a.m. and morning/noon: 8 a.m. to 2 p.m.) between the milking phases were not equally long, comparable numbers of values were available ($n = 91$ vs. 103). After the morning milking, the emissions decreased slightly for the first three hours followed by a slight increase. An almost opposite pattern could be found after the second milking in the afternoon.

4 Discussion

4.1 Flux data availability and selection

Fluxes used for cow emission calculations were less than 3 % of the total number of 30 min intervals (Table 1). In average years 3.6 ha of pasture are approximately sufficient to feed 20 dairy cows by rotational grazing during the early season. The cold and wet spring in 2013 negatively influenced the productivity of the pasture. Therefore, more than expected additional pasture time outside the study field was needed to feed the animals. These pastures were too far away to catch a signal by the EC tower, but were used for 44 % of the time. Hence the data coverage to measure cow emissions was lower than expected. The selection of acceptable wind directions and the limited

BGD
12, 3419–3468, 2015

probability that the wind came from the direction where the cows were actually grazing further reduced the number of cases selected as cow fluxes. Cow emissions with sufficient FP contribution mostly induced well defined peaks in the cross-covariance function (Fig. 3) and were well above the flux detection limit (similar as found by Detto et al., 2011). Even if the cows were grazing in the far paddocks 94 % of the fluxes already filtered by the other quality criteria were determined at dynamic lag times. This shows that a further quality filtering by a stationarity test was not needed.

Individual soil exchange fluxes were mostly below the (3σ) detection limit of $20\,\mathrm{nmol\,m^{-2}\,s^{-1}}$ and more than 92 % were determined at the fixed lag time. Baldocchi et al. (2012) reported a detectable limit of $\pm 4\,\mathrm{nmol\,m^{-2}\,s^{-1}}$ for a similar set up. The higher detection limit in this study has to be attributed to a different set-up but also to the stronger polluted region with various agricultural CH_4 sources (farm facilities). The uncertainty of the soil flux was of minor importance for the calculations of the cow emissions by the GPS and PAD methods (Eqs. 4 and 6), because the selected cow fluxes with significant FP contribution were about two orders of magnitude higher than $F_{\mathrm{soil}} = 4 \pm 3\,\mathrm{nmol\,m^{-2}\,s^{-1}}$ (Fig. 7). Obviously the selection of soil fluxes was possible only due to the GPS position information of the cows. Soil fluxes observed here are of similar magnitude like fluxes measured in other studies: CH_4 fluxes in the order of 0 to $10\,\mathrm{nmol\,m^{-2}\,s^{-1}}$ are reported from a drained and grazed peatland pasture (Baldocchi et al., 2012), fluxes around zero seldomly larger than $25\,\mathrm{nmol\,m^{-2}\,s^{-1}}$ for a grassland in Switzerland after renovation (Merbold et al., 2014), and fluxes between -1.3 and $9.6\,\mathrm{nmol\,m^{-2}\,s^{-1}}$ from a sheep grazed grassland measured by chambers (Dengel et al., 2011).

Methane fluxes from pasture always include fluxes from animal droppings (dung and urine). Therefore the soil fluxes referred to here are the combination of fluxes from the soil microbial community and fluxes from dung/urine which normally dominate over the pure soil fluxes (Flessa et al., 1996). Emissions from cattle dung are estimated to $0.778\,\mathrm{g\,CH_4\,head^{-1}}$ (Flessa et al., 1996) and from finish dairy cows to $470\,\mathrm{g\,CH_4\,ha^{-1}}$ over a 110 day grazing period (Maljanen et al., 2012). The soil flux in the present study

BGD
12, 3419–3468, 2015

($16\,g\,ha^{-1}\,d^{-1}$) is around three times higher than the corresponding flux calculated with the literature numbers (Flessa et al. (1996): $5\,g\,ha^{-1}\,d^{-1}$ and Maljanen et al. (2013): $4.3\,g\,ha^{-1}\,d^{-1}$) but in the same order of magnitude. Hence, the soil in the present study was a source of CH_4. Factors which may explain differences in the present study and the literature are different animal breeds/types, soil and vegetation types, and soil and weather conditions. Additionally the rotational grazing lead to measurements of mixed fluxes from old and new dung patches.

4.2 Source distance effect and footprint uncertainty

In the GPS and PAD method, cow emissions were derived from the measured fluxes (corrected for soil exchange) with the help of the KM01 footprint model (Eqs. 4 and 6). Although it can be assumed that the cows emitted the same amount of CH_4 whether they grazed in the far or the near paddocks, a systematic effect of their distance from the EC tower was found (cf. *near cows* vs. *far cows* results in Table 2). The accuracy of the emissions depends on the accuracy of the flux measurement and on the accuracy of the FP model. In general fluxes induced from cows further away were smaller (Fig. 7) and therefore tended to have a higher relative uncertainty than fluxes closer to the EC tower. Additionally the relative FP accuracy is assumed to be lower further away from the EC tower. This led to systematic larger uncertainties for calculations in the *far cows* case compared to the *near cows* case. One potential error source in the FP calculation could be the choice of z_0. The observed course of z_0 over the year (Fig. 8) coincides with the herbage productivity during the season and corresponds to around 1/10 of the grass height. The presence of the cows (in near paddocks) only slightly increased z_0 but the values remained in the expected range of 8 mm to 6 cm for short to long grass terrains (Wieringa, 1993). For occasional large obstacles (separated by at least 20 times the obstacle height) rather a value of 10 cm and larger is expected (WMO, 2008). Cows were moving obstacles in the FP. Larger effects seen for a fixed obstacle were obviously blurred if the obstacle moves. Additionally variations of the

BGD
12, 3419–3468, 2015

wind direction in a 30 min interval amplify the effect of moving. For the FP calculation we therefore generally limited z_0 to a certain range around the mean seasonal course. For the majority of the cases, individually calculated z_0 values lay within this range, but in a minor fraction (18 %) of the cases with cows, they exceeded the range (see Fig. 8) and were truncated to the upper range limit. We tested the effect of a doubling of the parameterized z_0 on Φ_{PAD} for the *near cows* case, as typically observed in Fig. 9, and found a moderate increase of around 17 % which would lower the calculated cow emissions proportionally. Because the truncation effect was small and only applied to few cases, we consider the uncertainty in z_0 as not important for our cow emission results. In particular it cannot explain the observed mean difference between *near* and *far cows* situations.

We chose the KM01 footprint model because the model uses an analytical solution and the calculation is fast compared to numerical particle models (e.g. backward Lagrangian stochastic models; bLS) which describe turbulence structure in a more complex way. Kljun et al. (2003) compared the KM01 model to a bLS model and found in general good agreements. However, the KM01 model underestimates the FP weight compared to the bLS model around the maximum of the FP function φ_{max} and overestimates the FP weight further downwind (see figures in Kljun et al., 2003). Integration over larger parts of the FP extension may balance this over-/underestimation.

The position of φ_{max} typically lay within 30 m of the EC tower (thus in PAD2 or PAD5). For cow positions between the tower and φ_{max} the KM01 model underestimates compared to the bLS model but overestimates after the maximum. Hence the over-/underestimation tended to be balanced for the *near cows* case. For the *far cows* case the KM01 model always overestimated the FP weights and thus the resulting emissions were underestimated on average. According to Kljun et al. (2003) the KM01 model also underestimates the FP weights in the direct vicinity of the EC tower (few meters). A detailed analysis of the cow positions (data not shown) revealed that in 68 % of the *near cows* cases animals were present in distances $< 2/3\varphi_{max}$ from the tower.

BGD
12, 3419–3468, 2015

But in less than 5 % of the cases more than a tenth of the 30 min was affected. Hence the influence on the $\overline{\varphi}_{\text{cow}}$ was generally small.

4.3 Comparison to published respiration chamber results

While measured methane EC fluxes depend on site and environmental conditions and are therefore not directly comparable to other studies, this is much better feasible for the average cow emissions derived by the GPS method and the two alternative methods (PAD and FIELD) described in Sects. 2.3–2.5. It can be assumed that dairy cows of similar breed and weight and with comparable productivity (milk yield) have a similar gross energy consumption and CH_4 emission. We therefore collected literature results from Swiss respiration chamber studies (Table 3) selected for a mean milk yield in the range of 20 to 25 $kg\,d^{-1}$ around the mean milk yield of the present study (22.7 $kg\,d^{-1}$). Most of these studies aimed to find diets that reduce CH_4 emission based on different forage types and supplements. Cow diets therefore vary between all studies but always fulfilled animal nutrient requirements. One value from van Dorland et al. (2006) which showed very low CH_4 emissions due to special diet supplements was excluded from Table 3. Mean body weight of cows in the present study (640 kg) was in the upper range of body weight in the selected chamber measurements.

Mean CH_4 emission over all selected studies of 404 $g\,CH_4\,head^{-1}\,d^{-1}$ agrees very well with emission measured by EC for the *near cows* cases (difference of only 5 %, within uncertainty range of EC results). The deviation for the PAD *near cows* results is about twice as large. The *far cows* results for GPS and PAD methods show even larger but negative deviations from the literature mean. The result of the FIELD method applied to the entire grazing period also shows a good agreement but we consider that as rather coincidental, because the estimated uncertainty of monthly values as well as the deviation of their mean and median is much larger.

Based on the FP uncertainty considerations in Sect. 4.2 and the agreement with the recent literature values, we consider the GPS *near cows* results as the most reliable in this study. They were derived from only large fluxes with relatively low uncertainty.

Therefore, the following discussion focusses on the GPS *near cows* results and uses them as reference for the comparison with the other results.

4.4 Systematic and random-like variations of cow emission

Our result show only a moderate diel cycle (Fig. 11) with highest emissions in the evening and lowest before noon (hourly means ±30 % around overall mean). Increasing emission fluxes during daytime hours were also found over a sheep pasture by Dengel et al. (2011). But their nighttime fluxes were much smaller (close to zero) compared to daytime. Laubach et al. (2013) observed maximum CH_4 emissions within two hours after maximum feeding activity of cattle. Those cattle were fed before noon with imported fodder (i.e. all animals fed at the same time) whereas the cows in the present study were free in choosing their grazing activity time over the entire day. Obviously this is reflected in the less pronounced diel cycle.

To assess and interpret potential systematic effects of variations in cow performance (among animals in the herd and with time over the grazing season) we used published emission models based on observed productivity parameters (see Ellis et al., 2010). Figure 12 compares the results of two models (Corré, 2002; Kirchgessner et al., 1995) estimating cow emission from recorded milk yield and body weight with results of this study. Although milk yield showed a general decrease over the first three months and a considerable variability within the herd, the effect on CH_4 emissions according to the models was relatively small. The observed monthly emissions showed a larger variability which cannot be explained by the variability of the cow performance.

Although the mean emissions observed in this study agree well with literature values the variation of the individual 30 min emissions is large (relative SD of 41 % for GPS *near cows*, see Table 2). It is a combination of various effects with major contributions of the discussed diel variation, the stochastic uncertainty (short term variability) of turbulence, and the changing source distribution (various numbers of cows in the FP and moving). Very similar relative variability of 30 min fluxes was reported in a study using the micrometeorological bLS method (Laubach et al., 2014). Similar to Laubach et al.

BGD
12, 3419–3468, 2015

(2014) the large scatter of our individual emission values showed a fairly random-like (normal) distribution (Fig. 13) with only minor deviation between mean and median. This distribution is clearly more symmetric than the corresponding distribution of cow FP weights (Fig. 10a). Based on this behavior, the estimated uncertainty range of the overall mean cow emission calculated according to Gaussian error propagation rules is considered as representative.

4.5 Relevance of cow position information

In an intensive rotational grazing system the cows are expected to effectively graze the entire paddock area. On shorter timescales of 30 min (Fig. 6) this assumption is often not fulfilled. For a grazing rotation phase of two days the example in Fig. 14a shows that the cows indeed visited the entire paddock, but their position distribution was not uniform with higher densities in the central part of the paddock. Even over the entire grazing season some inhomogeneity in the cow density distribution persisted (Fig. 14b). Despite this inhomogeneity the mean emission calculated with the PAD method (implicitly assuming homogeneous cow distribution within the paddock) was comparable to the emission based on GPS data (Table 2), yet with a larger uncertainty range. Thus the hypothesis that more detailed information lead to better results was not clearly verified in this case. Apparently the limited size and the geometric arrangement of the paddocks in relation to typical extension of the FP area in the main wind sectors limited the value of the more detailed GPS information.

The PAD method uses a similar level of cow position information as other micrometeorological experiments applying the bLS approach (Laubach et al., 2008, 2013; Laubach and Kelliher, 2005; McGinn et al., 2011). The bLS models use the geometry of the fenced grazing area and perform a concentration FP calculation (instead of the flux FP used here). The size of the animal containing fenced areas in those experiments (0.1 to 2 ha) were of the same order of magnitude as the paddock size in this study. Although the density of grazing animals in Laubach et al. (2013) was five times higher than the average density of 33 heads ha^{-1} in this study, they reported

BGD
12, 3419–3468, 2015

systematic effects of uneven cow distribution within the grazing area on derived mean cow emissions. They found a discrepancy of up to +68 % between their reference SF_6 technique and the bLS model using concentration profile measurements at a single mast. The bLS experiments with line-averaging concentration measurements yielded generally better results because they are less sensitive to the source distribution. The corresponding uncertainties were similar to uncertainties found in this study.

Although some inhomogeneity of the animal density was found within the paddocks, the rotational grazing system prevented major differences among them on the long term (Fig. 14b). This may not be the case for a free range grazing system without subdivision of the field into paddocks, like e.g. in the study by Dengel et al. (2011). In such a case, a larger scale inhomogeneity may develop leading to a systematic under- or overrepresentation of the animals in the flux FP (in the main wind sectors), and the FIELD method without cow position information would yield biased results. As an alternative to the use of GPS sensors on individual animals, their position could be monitored by the use of digital cameras and animal detection software (Baldocchi et al., 2012).

The problem discussed so far for CH_4 also exists for the investigation of CO_2 flux measurements at pasture sites, because of the considerable contribution of animal respiration to the net ecosystem exchange. If joint CO_2 and CH_4 fluxes are available at the site CH_4 can be used as a tracer for ruminant induced CO_2 fluxes by using typical CH_4/CO_2 ratios of exhaled air found in respiration chamber measurements.

5 Conclusions

EC flux and GPS data were combined using an analytical FP model to derive animal related CH_4 emissions. With an adjusted evaluation procedure (no de-spiking nor stationarity selection) an underestimation or rejection of cases with strong cow signals could be avoided. A systematic effect of the distance from the EC tower to the source (cows) was found, which has to be attributed to the applied analytical FP model. It over-

BGD
12, 3419–3468, 2015

estimates the FP weight of sources in large distances (> 25 times the measurement height). The problem may be avoided by using a more sophisticated Lagrangian dispersion model. The roughness length z_0 used as input for the FP model was moderately but systematically increased by the cows which should be taken into account.

The position information allowed a reliable distinction of fluxes representing soil exchange without direct influence of cows. Although these fluxes were very low with marginal effect on the determination of cow emissions (using cow position information), they are potentially more important for the annual CH_4 and full GHG budget of the pasture. In our rotational grazing set up, the simple information on paddock occupation times led to comparable estimates of mean cow emissions like the more detailed GPS information. For other pasture flux sites with a different grazing system, cow position information may be more crucial to determine representative animal emissions and soil exchange fluxes. We conclude that EC measurements over pasture are sufficiently accurate to estimate mean CH_4 emissions of grazing animals. Although the uncertainty makes it difficult to detect small differences in animal CH_4 emissions during short-term experiments, the EC method is well suitable for assessing longer-term ecosystem GHG budgets that are necessary to improve national inventories.

Acknowledgements. We gratefully acknowledge the funding from the Swiss National Science Foundation (Grant No. 205 321_138 300). We wish to thank Hubert Bollhalder, Roman Gubler, Veronika Wolff, Andreas Rohner, Manuel Schuler, Markus Jocher, Manuela Falk, Lukas Eggerschwiler and Bernard Papaux for support with the sensors and in the field. We thank Daniel Bretscher for the collection of studies containing data of respiration chamber measurements and the discussion of these data, Robin Giger for graphical help with figures, and Jörg Sintermann for provision of R code.

References

Ammann, C., Brunner, A., Spirig, C., and Neftel, A.: Technical note: water vapour concentration and flux measurements with PTR-MS, J. Environ. Qual., 6, 4643–4651, 2006.

Arrigo, Y., Chaubert, C., Daccord, R., Gagnaux, D., Gerber, H., Guidon, D., Jans, F., Kessler, J., Lehmann, E., Morel, I., Münger, A., Rouel, M., and Wyss, U.: Fütterungsempfehlungen und Nährwerttabellen für Wiederkäuer: das grüne Buch, 4th edn., Eidgenössische Forschungsanstalt für Nutztiere, Zollikofen, Switzerland, 1999.

Aubinet, M., Grelle, A., Ibrom, A., Rannik, Ü., Moncrieff, J., Foken, T., Kowalski, A. S., Martin, P. H., Berbigier, P., Bernhofer, C., Clement, R., Elbers, J., Granier, A., Gruenwald, T., Morgenstern, K., Pilegaard, K., Rebmann, C., Snijders, W., Valentini, R., and Vesala, T.: Estimates of the annual net carbon and water exchange of forests: the EUROFLUX methodology, Adv. Ecol. Res., 30, 113–175, 2000.

Baer, D. S., Paul, J. B., Gupta, M., and O'Keefe, A.: Sensitive absorption measurements in the near-infrared region using off-axis integrated-cavity-output spectroscopy, Appl. Phys. B-Lasers O., 75, 261–265, doi:10.1007/s00340-002-0971-z, 2002.

Baldocchi, D. D.: Assessing the eddy covariance technique for evaluating carbon dioxide exchange rates of ecosystems: past, present and future, Glob. Change Biol., 9, 479–492, 2003.

Baldocchi, D. D., Detto, M., Sonnentag, O., Verfaillie, J., Teh, Y. A., Silver, W., and Kelly, N. M.: The challenges of measuring methane fluxes and concentrations over a peatland pasture, Agr. Forest Meteorol., 153, 177–187, doi:10.1016/j.agrformet.2011.04.013, 2012.

Corré, W. J.: Agricultural Land Use and Emissions of Methane and Nitrous Oxide in Europe, Report 40, Plant Research International, Wageningen, 2002.

Dabberdt, W. F., Lenschow, D. H., Horst, T. W., Zimmermann, P. R., Oncley, S. P., and Delany, A. C.: Atmosphere–surface exchange measurements, Science, 260, 1472–1481, 1993.

Dengel, S., Levy, P. E., Grace, J., Jones, S. K., and Skiba, U. M.: Methane emissions from sheep pasture, measured with an open-path eddy covariance system, Glob. Change Biol., 17, 3524–3533, doi:10.1111/j.1365-2486.2011.02466.x, 2011.

Detto, M., Verfaillie, J., Anderson, F., Xu, L., and Baldocchi, D.: Comparing laser-based open- and closed-path gas analyzers to measure methane fluxes using the eddy covariance method, Agr. Forest Meteorol., 151, 1312–1324, doi:10.1016/j.agrformet.2011.05.014, 2011.

Ellis, J. L., Bannink, A., France, J., Kebreab, E., and Dijkstra, J.: Evaluation of enteric methane prediction equations for dairy cows used in whole farm models: methane prediction in vivo farm models, Glob. Change Biol., 16, 3246–3256, doi:10.1111/j.1365-2486.2010.02188.x, 2010.

BGD
12, 3419–3468, 2015

Eddy covariance methane flux measurements over a grazed pasture

R. Felber et al.

Flessa, H., Dörsch, P., Beese, F., König, H., and Bouwman, A. F.: Influence of cattle wastes on nitrous oxide and methane fluxes in pasture land, J. Environ. Qual., 25, 1366–1370, doi:10.2134/jeq1996.00472425002500060028x, 1996.
Foken, T., Aubinet, M., and Leuning, R.: The eddy covariance method, in: Eddy Covariance, edited by: Aubinet, M., Vesala, T., and Papale, D., Springer, Dordrecht, the Netherlands, 1–19, 2012a.
Foken, T., Leuning, R., Oncley, S. R., Mauder, M., and Aubinet, M.: Corrections and data quality control, in: Eddy Covariance, edited by: Aubinet, M., Vesala, T., and Papale, D., Springer, Dordrecht, the Netherlands, 85–131, 2012b.
Graf, A., van de Boer, A., Moene, A., and Vereecken, H.: Intercomparison of methods for the simultaneous estimation of zero-plane displacement and aerodynamic roughness length from single-level eddy-covariance data, Bound.-Lay. Meteorol., 151, 373–387, doi:10.1007/s10546-013-9905-z, 2014.
Harper, L. A., Denmead, O. T., Freney, J. R., and Byers, F. M.: Direct measurements of methane emissions from grazing and feedlot cattle, J. Anim. Sci., 77, 1392–1401, 1999.
Hiller, R. V., Bretscher, D., DelSontro, T., Diem, T., Eugster, W., Henneberger, R., Hobi, S., Hodson, E., Imer, D., Kreuzer, M., Künzle, T., Merbold, L., Niklaus, P. A., Rihm, B., Schellenberger, A., Schroth, M. H., Schubert, C. J., Siegrist, H., Stieger, J., Buchmann, N., and Brunner, D.: Anthropogenic and natural methane fluxes in Switzerland synthesized within a spatially explicit inventory, Biogeosciences, 11, 1941–1959, doi:10.5194/bg-11-1941-2014, 2014.
Hindrichsen, I. K., Wettstein, H.-R., Machmüller, A., Knudsen, K. E. B., Madsen, J., and Kreuzer, M.: Digestive and metabolic utilisation of dairy cows supplemented with concentrates characterised by different carbohydrates, Anim. Feed Sci. Tech., 126, 43–61, doi:10.1016/j.anifeedsci.2005.06.004, 2006a.
Hindrichsen, I. K., Wettstein, H.-R., Machmüller, A., and Kreuzer, M.: Methane emission, nutrient degradation and nitrogen turnover in dairy cows and their slurry at different milk production scenarios with and without concentrate supplementation, Agr. Ecosyst. Environ., 113, 150–161, doi:10.1016/j.agee.2005.09.004, 2006b.
Kaimal, J. C. and Finnigan, J. J.: Atmospheric Boundary Layer Flows?, Their Structure and Measurement, Oxford University Press, New York, 1994.
Kirchgessner, M., Windisch, W., and Müller, H. L.: Nutritional factors affecting methane production by ruminants, in: Ruminant Physiology: Digestion, Metabolism, Growth and Reproduc-

BGD
12, 3419–3468, 2015

tion, edited by: Engelhardt, W. V., Leonhard-Mare, S., Breve, G., and Giesecke, D., Ferdinand Enke Verlag, Stuttgart, 333–343, 1995.

Kljun, N., Kormann, R., Rotach, M. W., and Meixer, F. X.: Comparison of the Langrangian Footprint, Bound.-Lay. Meteorol., 106, 349–355, 2003.

Kormann, R. and Meixner, F. X.: An analytical footprint model for non-neutral stratification, Bound.-Lay. Meteorol., 99, 207–224, 2001.

Lassey, K. R.: Livestock methane emission: from the individual grazing animal through national inventories to the global methane cycle, Agr. Forest Meteorol., 142, 120–132, doi:10.1016/j.agrformet.2006.03.028, 2007.

Laubach, J. and Kelliher, F. M.: Methane emissions from dairy cows: comparing open-path laser measurements to profile-based techniques, Agr. Forest Meteorol., 135, 340–345, doi:10.1016/j.agrformet.2005.11.014, 2005.

Laubach, J., Kelliher, F. M., Knight, T. W., Clark, H., Molano, G., and Cavanagh, A.: Methane emissions from beef cattle – a comparison of paddock- and animal-scale measurements, Aust. J. Exp. Agr., 48, 132, doi:10.1071/EA07256, 2008.

Laubach, J., Bai, M., Pinares-Patiño, C. S., Phillips, F. A., Naylor, T. A., Molano, G., Cárdenas Rocha, E. A., and Griffith, D. W. T.: Accuracy of micrometeorological techniques for detecting a change in methane emissions from a herd of cattle, Agr. Forest Meteorol., 176, 50–63, doi:10.1016/j.agrformet.2013.03.006, 2013.

Laubach, J., Grover, S. P. P., Pinares-Patiño, C. S., and Molano, G.: A micrometeorological technique for detecting small differences in methane emissions from two groups of cattle, Atmos. Environ., 98, 599–606, doi:10.1016/j.atmosenv.2014.09.036, 2014.

Leuning, R., Baker, S. K., Jamie, I. M., Hsu, C. H., Klein, L., Denmead, O. T., and Griffith, D. W. T.: Methane emission from free-ranging sheep: a comparison of two measurement methods, Atmos. Environ., 33, 1357–1365, 1999.

Maljanen, M. E., Virkajärvi, P., and Martikainen, P.: Dairy cow excreta patches change the boreal grass swards from sink to source of methane, Agr. Food Sci., 21, 91–99, 2012.

McGinn, S. M., Turner, D., Tomkins, N., Charmley, E., Bishop-Hurley, G., and Chen, D.: Methane emissions from grazing cattle using point-source dispersion, J. Environ. Qual., 40, 22, doi:10.2134/jeq2010.0239, 2011.

Merbold, L., Eugster, W., Stieger, J., Zahniser, M., Nelson, D., and Buchmann, N.: Greenhouse gas budget (CO_2, CH_4 and N_2O) of intensively managed grassland following restoration, Glob. Change Biol., 20, 1913–1928, doi:10.1111/gcb.12518, 2014.

BGD
12, 3419–3468, 2015

MeteoSchweiz: GRA_norm8110.pdf, available at: http://www.meteoswiss.admin.ch/files/kd/climsheet/de/GRA_norm8110.pdf (last access: 13 October 2014), 2014.

Moore, C. J.: Frequency response corrections for eddy correlation systems, Bound.-Lay. Meteorol., 37, 17–35, 1986.

Münger, A. and Kreuzer, M.: Methane emission as determined in contrasting dairy cattle breeds over the reproduction cycle, Int. Congr. Ser., 1293, 119–122, doi:10.1016/j.ics.2006.01.072, 2006.

Münger, A. and Kreuzer, M.: Absence of persistent methane emission differences in three breeds of dairy cows, Aust. J. Exp. Agr., 48, 77, doi:10.1071/EA07219, 2008.

Munger, J. W., Loescher, H. W., and Luo, H.: Measurement, tower, and site design considerations, in: Eddy Covariance, edited by: Aubinet, M., Vesala, T., and Papale, D., Springer, Dordrecht, the Netherlands, 21–58, 2012.

Myhre, G., Shindell, D., Béron, F.-M., Collins, W., Fuglestvedt, J., Huang, J., Koch, D., Lamarque, J.-F., Lee, D., Mendoza, B., Nakajima, T., Robock, A., Stephens, G., Takemura, T., and Zhang, H.: Anthropogenic and natural radiative forcing, in: Climate Change 2013, The Physical Science Basis, Contribution of Working Group I to the Fifth Assessment Report of the Intergovernmental Panel on Climate Change, edited by: Stocker, T. F., Qin, D., Plattner, G.-K., Tignor, M., Allen, S. K., Boschung, J., Nauels, A., Xia, Y., Bex, V., and Midgle, P. M., Cambridge University Press, Cambridge, UK and New York, NY, USA, 659–740, 2013.

Neftel, A., Spirig, C., and Ammann, C.: Application and test of a simple tool for operational footprint evaluations, Environ. Pollut., 152, 644–652, doi:10.1016/j.envpol.2007.06.062, 2008.

Peltola, O., Mammarella, I., Haapanala, S., Burba, G., and Vesala, T.: Field intercomparison of four methane gas analyzers suitable for eddy covariance flux measurements, Biogeosciences, 10, 3749–3765, doi:10.5194/bg-10-3749-2013, 2013.

Pinares-Patiño, C. S., D'Hour, P., Jouany, J.-P., and Martin, C.: Effects of stocking rate on methane and carbon dioxide emissions from grazing cattle, Agr. Ecosyst. Environ., 121, 30–46, doi:10.1016/j.agee.2006.03.024, 2007.

R Core Team: R: a Language and Environment For Statistical Computing, R Foundation for Statistical Computing, Vienna, Austria, available at: http://www.R-project.org/, 20 March 2014.

Schmid, H. P., Grimmond, C. S. B., Cropley, F., Offerle, B., and Su, H.-B.: Measurements of CO_2 and energy fluxes over a mixed hardwood forest in the mid-western United States, Agr. Forest Meteorol., 103, 357–374, 2000.

Smith, P., Martino, D., Cai, Z., Gwary, D., Janzen, H., Kumar, P., McCarl, B., Ogle, S., O'Mara, F., Rice, C., Scholes, B., and Sirotenko, O.: Agriculture, in: Climate Change 2007: Mitigation, Contribution of Working Group III to the Fourth Assessment Report of the Intergovernmental Panel on Climate Change, edited by: Metz, B., Davidson, O. R., Bosch, P. R., Dave, R., and Meyer, L. A., Cambridge University Press, Cambridge, UK and New York, NY, USA, 497–540, 2007.

Tuzson, B., Hiller, R. V., Zeyer, K., Eugster, W., Neftel, A., Ammann, C., and Emmenegger, L.: Field intercomparison of two optical analyzers for CH_4 eddy covariance flux measurements, Atmos. Meas. Tech., 3, 1519–1531, doi:10.5194/amt-3-1519-2010, 2010.

Van Dorland, H. A., Wettstein, H.-R., Leuenberger, H., and Kreuzer, M.: Comparison of fresh and ensiled white and red clover added to ryegrass on energy and protein utilization of lactating cows, Anim. Sci., 82, 691, doi:10.1079/ASC200685, 2006.

Van Dorland, H. A., Wettstein, H.-R., Leuenberger, H., and Kreuzer, M.: Effect of supplementation of fresh and ensiled clovers to ryegrass on nitrogen loss and methane emission of dairy cows, Livest. Sci., 111, 57–69, doi:10.1016/j.livsci.2006.11.015, 2007.

Webb, E. K., Pearman, G. I., and Leuning, R.: Correction of flux measurements for density effects due to heat and water vapour transfer, Q. J. Roy. Meteor. Soc., 106, 85–100, 1980.

Wieringa, J.: Representative roughness parameters for homogeneous terrain, Bound.-Lay. Meteorol., 63, 323–363, 1993.

Witte, T. H. and Wilson, A. M.: Accuracy of WAAS-enabled GPS for the determination of position and speed over ground, J. Biomech., 38, 1717–1722, doi:10.1016/j.jbiomech.2004.07.028, 2005.

WMO: Guide to Meteorological Instruments and Methods of Observation, World Meteorological Organization, Geneva, Switzerland, 2008.

BGD

12, 3419–3468, 2015

Eddy covariance methane flux measurements over a grazed pasture

R. Felber et al.

Table 1. Number of available 30 min CH_4 fluxes after the application of selection criteria for the three calculation methods (FIELD, GPS, and PAD method). Bold numbers were used for final calculations.

	all/FIELD	GPS			PAD	
		soil	*near cows*	*far cows*	*near cows*	*far cows*
grazing season[1]	10 080					
quality operation[2]	9856					
quality turbulence[3]	7093					
wind direction[4]	4645					
flux error/LoD[5]	**3630**					
soil/cow attrib.[6]		2076	205	64	216	74
outliers[7]		**1917**	**194**	**63**	**198**	**74**

[1] Total number of 30 min intervals in grazing season (9 April–4 November 2013).
[2] Available data with proper instrument operation (hard flags < 10).
[3] Acceptable quality of turbulence parameters and vertical tilt angle between −2 and 6°.
[4] Accepted (undisturbed) wind direction: 25 to 135° and 195 to 265°.
[5] No fluxes at fixed lag if flux larger than flux detection limit (LoD).
[6] Split fluxes based on GPS data; exclusion of intervals with low GPS data coverage; exclusion of intervals (730) when cows were moved between barn and pasture; discarding of cases with intermediate mean cow FP weights.
[7] Soil flux outliers removed; cow fluxes removed based on emission (E_{cow}) outliers.

BGD
12, 3419–3468, 2015

Table 2. Methane emissions calculated with known cow position (GPS), based on knowledge of paddock (PAD), and without cow position information (FIELD) for different distances of the cow herd to the EC tower (*near*, *far*). All values, except *n*, are in units $g\,CH_4\,head^{-1}\,d^{-1}$.

	GPS		PAD		FIELD
	near cows	*far cows*	*near cows*	*far cows*	
Mean	423	286	443	319	389[a]/470[b]
±2 SE	±24	±32	±32	±40	±184[b]
Median	408	296	405	323	348[b]
SD	168	124	226	173	243[b]
n	194	63	198	74	7[b]

[a] Mean of the FIELD method represents an integral (arithmetic mean) over the entire grazing period.
[b] Statistics calculated based on monthly results (April–October).

BGD
12, 3419–3468, 2015

Table 3. Methane emissions from open-circuit respiration chamber measurements of Holstein and Swiss Brown breeds selected for milk yields and body weights comparable to cows in the present study. Hindrichsen et al. (2006a) used Swiss Brown breeds only.

Reference	Emission [$g\,CH_4\,head^{-1}\,d^{-1}$]	Body weight [kg]	ECM[1] [$kg\,d^{-1}$]
van Dorland et al. (2006)	428	669	23.5
van Dorland et al. (2006)	413	669	24.4
van Dorland et al. (2007)	424	641	24.5
Hindrichsen et al. (2006a)	415	586	20.0
Hindrichsen et al. (2006a)	379	583	20.0
Hindrichsen et al. (2006a)	374	594	21.0
Hindrichsen et al. (2006b)	414	619	22.8
Münger and Kreuzer (2006)[2]	387	593	22.9
mean	404	619	22.4
SD	21	36	1.8

[1] ECM: energy-corrected milk yield.
[2] Mean values of lactation week 8, 15, and 23.

BGD
12, 3419–3468, 2015

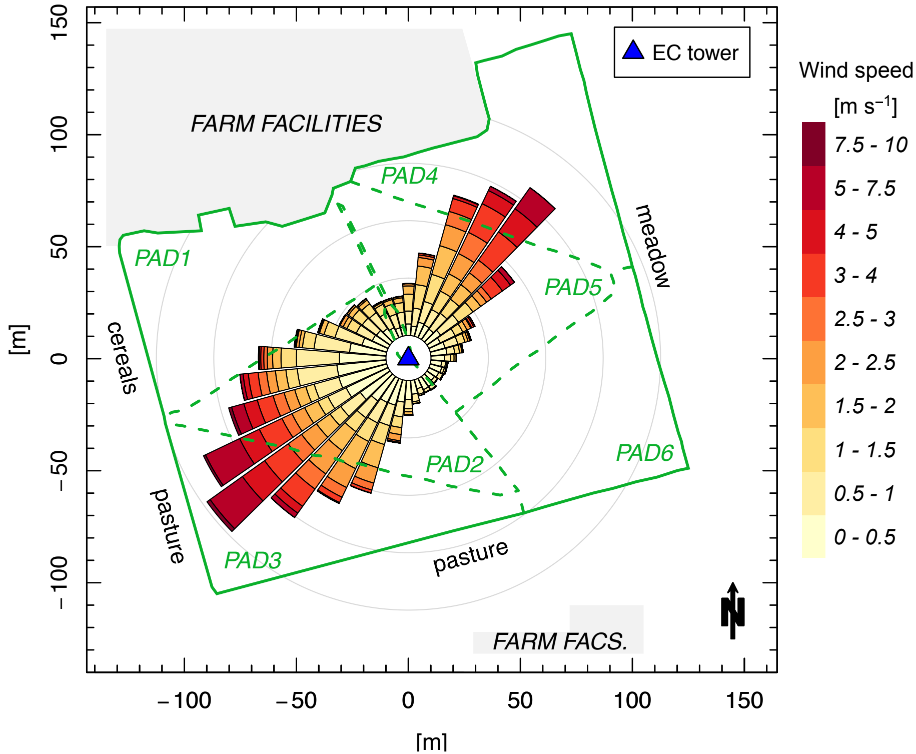

Figure 1. Plan of the measurement site with the pasture (solid green line) and its division into six paddocks PAD1 to PAD6 (dashed green lines) used for rotational grazing. Around the EC tower in the center, the wind direction distribution for the year 2013 is indicated with a resolution of 10°. The gray circles indicate sector contributions of 2, 4, 6, and 8 % (from inside outwards). Each sector is divided into color shades indicating the occurrence of wind speed classes (see legend).

BGD
12, 3419–3468, 2015

Title Page
Abstract | Introduction
Conclusions | References
Tables | Figures
◀◀ | ▶▶
◀ | ▶
Back | Close
Full Screen / Esc
Printer-friendly Version
Interactive Discussion

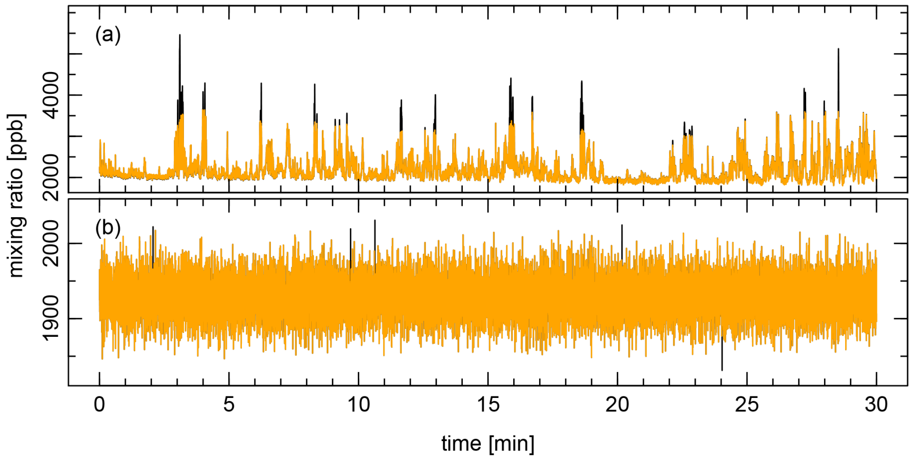

Figure 2. 10 Hz time series of CH_4 mixing ratio of 15 June 2013 for two exemplary 30 min intervals **(a)** with and **(b)** without cows in the FP. In black untreated data, in orange data after de-spiking. The two cases correspond to the cross-covariance functions in Fig. 3a and b.

BGD
12, 3419–3468, 2015

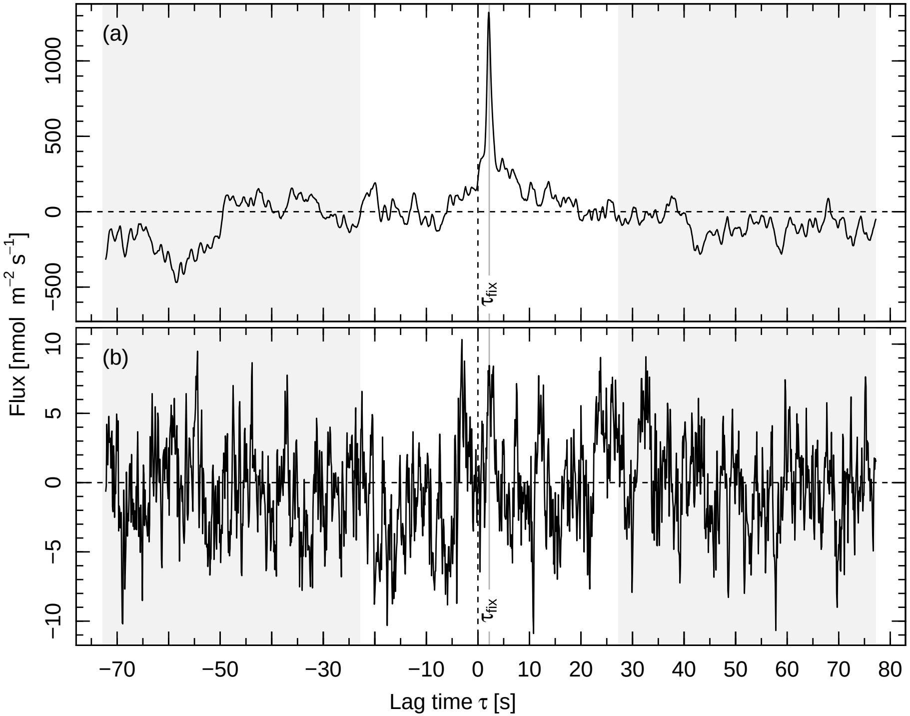

Figure 3. Cross-covariance function of CH_4 fluxes for two 30 min intervals of 15 June 2013 **(a)** with and **(b)** without cows in the footprint. The panels correspond to the intervals in Fig. 2. τ_{fix} indicates the expected fixed lag time for the EC system. The gray areas on both sides indicate the ranges used for estimating the flux uncertainty and detection limit.

BGD
12, 3419–3468, 2015

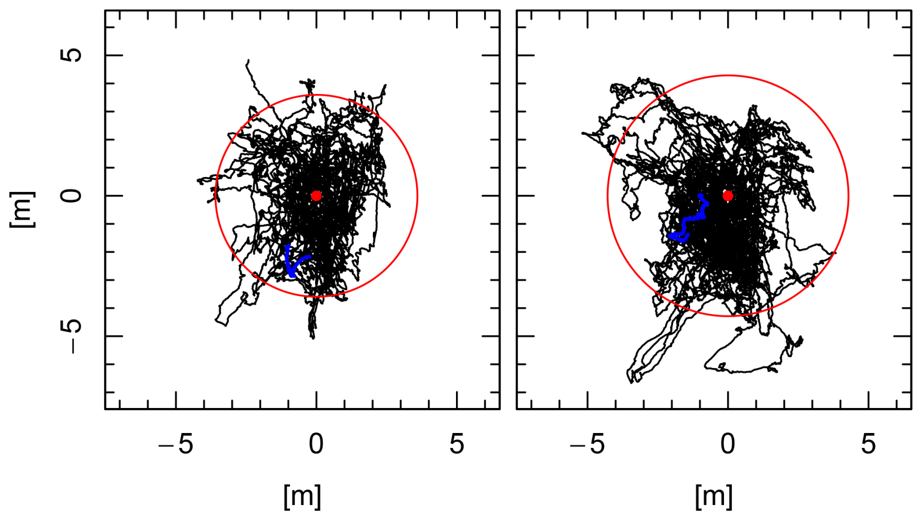

Figure 4. Two example results of the GPS device side-by-side fixed point accuracy test during five consecutive days. Each device showed an individual variability of the measured position with time, not correlated to other devices. The blue line indicates data points of one 30 min interval. The central red point indicates the average position over time and all devices. The distance comprising 95 % of all data points (red circle) varied for all tested devices from 1.9 to 4.3 m.

BGD
12, 3419–3468, 2015

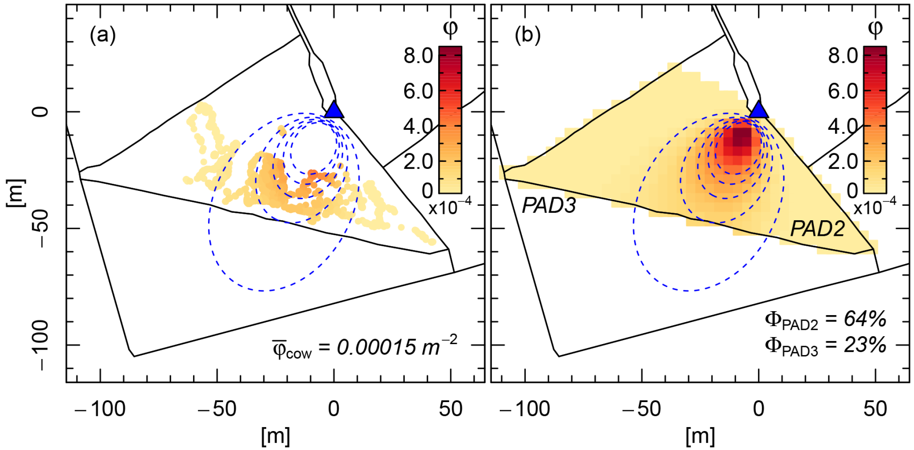

Figure 5. Determination of footprint weights for a cow herd in PAD2 during a 30 min interval with two different approaches: **(a)** "GPS method" (Eq. 3) based on the actual cow positions. The color indicates the weight of each GPS point to the measured flux; **(b)** "PAD method" (Eq. 5) calculating the area integrated footprint weight of the entire paddock area (here: Φ_{PAD2} = 64 %). The color of each pixel (4 m × 4 m grid) indicates the footprint weight. The blue triangle indicates the position of the EC tower and the blue dashed lines are isolines of the footprint weight function.

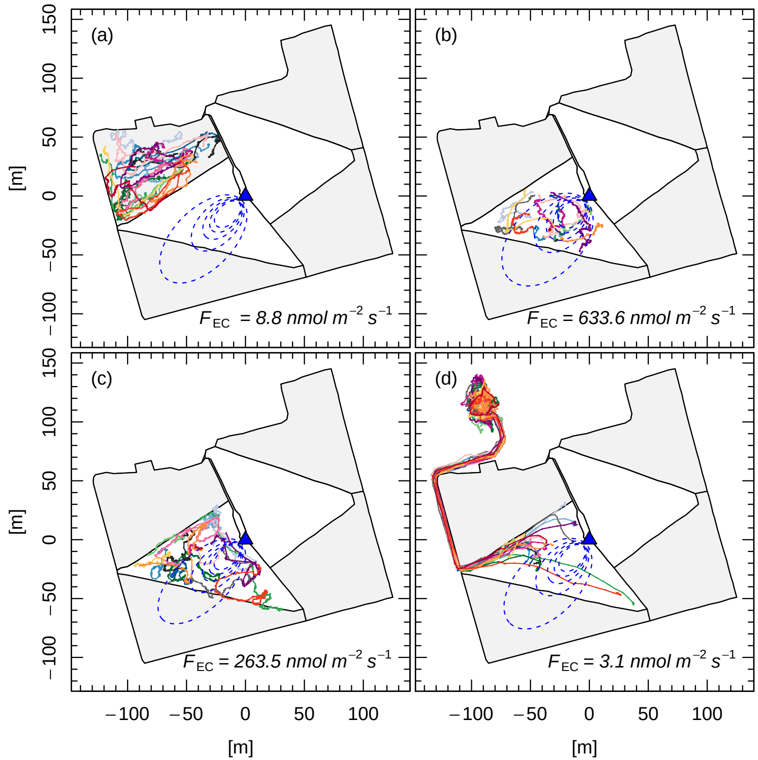

Figure 6. Four examples of 30 min intervals with similar wind and footprint conditions (blue isolines) but different cow distribution and observed fluxes (F_{EC}). For each cow, the GPS registered position (5 s resolution over 30 min) is marked with a line of individual color. Paddocks representing *near cows* situations are white and *far cows* are gray. **(a)** no cows in the footprint, i.e. soil fluxes are measured, **(b–d)** the higher the number and residence time of cows in the footprint the larger the observed flux.

BGD
12, 3419–3468, 2015

Eddy covariance methane flux measurements over a grazed pasture

R. Felber et al.

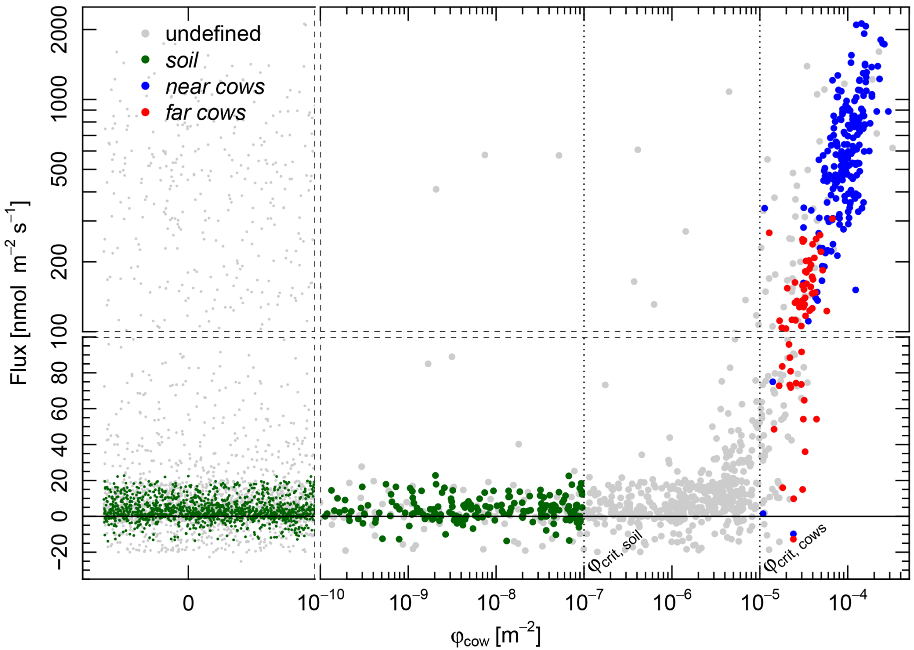

Figure 7. Quality selected 30 min CH_4 fluxes plotted against the mean cow footprint weight ($\overline{\varphi}_{cow}$). Cases with zero $\overline{\varphi}_{cow}$ (most of the diagram) were randomly scattered horizontally for better visualization. Cases used for soil flux and cow emission calculation are marked in color. Points in gray correspond to selected fluxes before the attribution into soil and cow fluxes and outlier removal.

BGD
12, 3419–3468, 2015

Eddy covariance methane flux measurements over a grazed pasture

R. Felber et al.

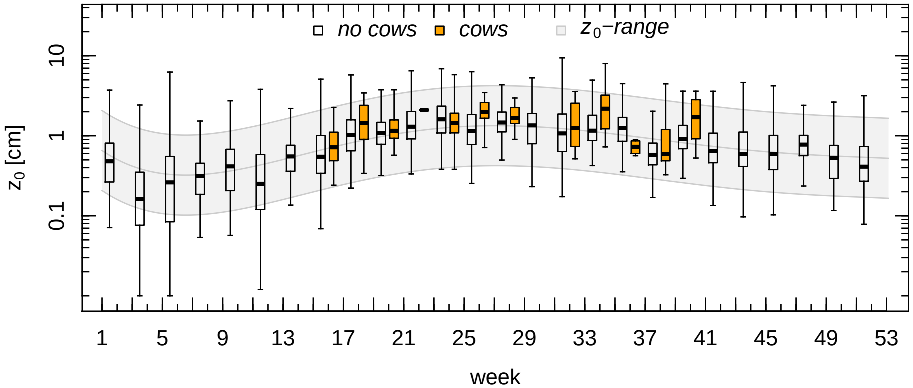

Figure 8. Bi-weekly distributions (boxplots) of calculated roughness length (z_0) for wind speeds $> 1.5\,\mathrm{m\,s^{-1}}$ separated for cases with no cows in the FP (white boxes) and cases with cows present in the FP (orange). Whiskers for the cow cases cover the full data range, outliers for no cows cases are not shown. The gray area indicates the z_0-range where the 30 min z_0 value was accepted for FP evaluation. The middle curve in the gray range represents the 6th order polynomial fit to the values without cows.

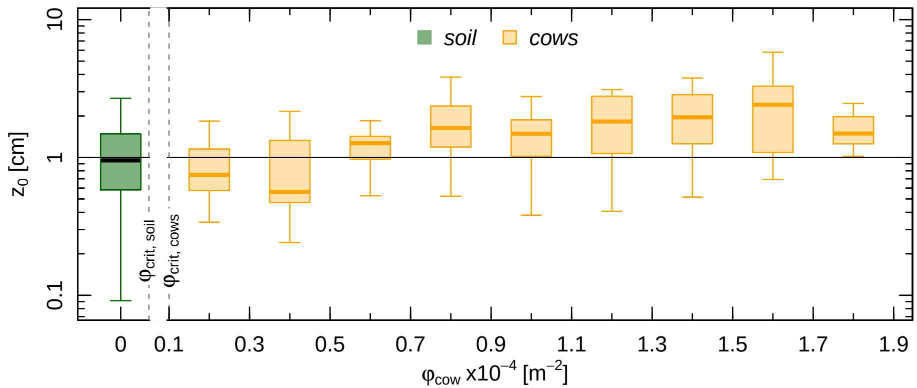

Figure 9. Effect of cows on roughness length (z_0). Boxplots of 30 min z_0 values determined by Eq. (2) for $\overline{u} > 1.5\,m\,s^{-1}$ as a function of average footprint weight of the cow herd ($\overline{\varphi}_{cow}$) base on GPS data. Whiskers cover the full data range. Orange for situation with cows, green for situation with no cows in the footprint.

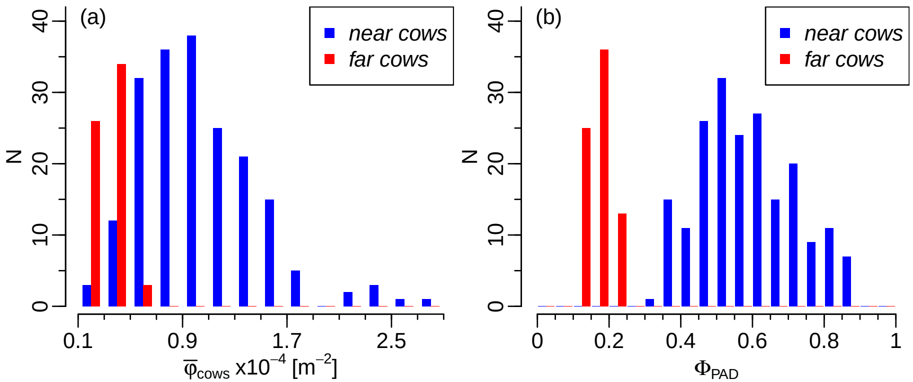

Figure 10. Histogram of footprint contributions **(a)** of cow positions used in the GPS method and **(b)** of occupied paddock area used in the PAD method. Cases are separated for distance of the cow herd from the EC tower in *near cows* and *far cows*.

BGD
12, 3419–3468, 2015

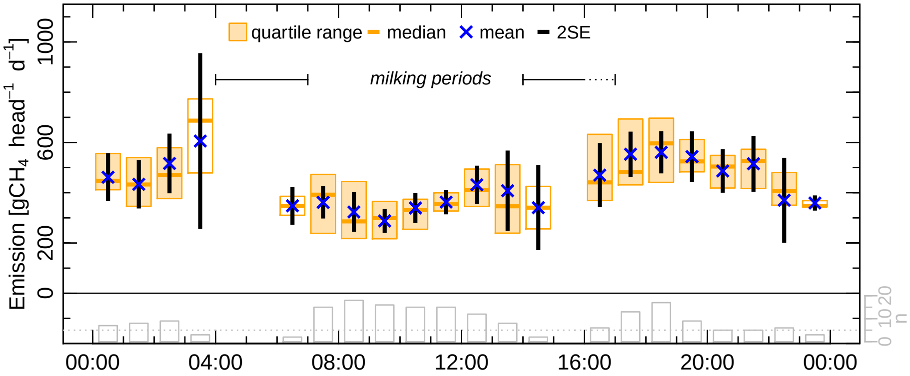

Figure 11. Average diel variation of CH_4 cow emissions for the *near cows* case. White quartile range boxes indicate hours where less than five values are available. The uncertainty is given as 2× SE (black lines). White bars (bottom) show the number of values for each hour (right axis). The two gaps indicate the time when the cows were in the barn for milking. The dashed line in the second milking period indicates that the cows sometimes stayed longer in the barn.

BGD
12, 3419–3468, 2015

Eddy covariance methane flux measurements over a grazed pasture

R. Felber et al.

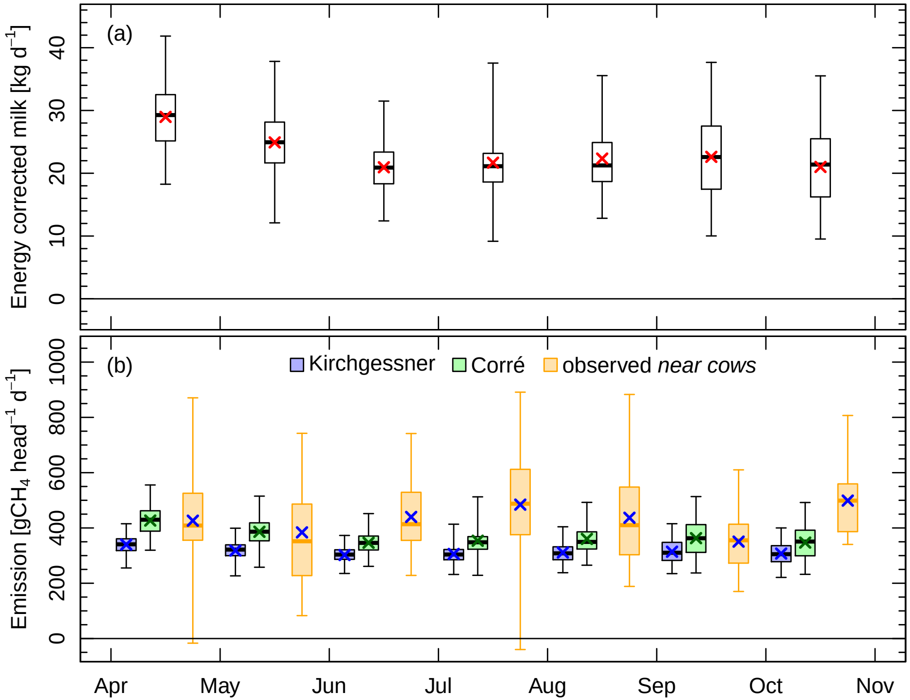

Figure 12. Monthly aggregated distribution of **(a)** energy-corrected daily milk yield (ECM) of the individual cows in the herd, and **(b)** cow methane emission as observed in this study (*near cows* cases) and modeled as a function of *ECM* and cow body weight (m) according to $10 + 4.9 \times \mathrm{ECM} + 1.5 \times m^{0.75}$ (Kirchgessner et al., 1995) and $(50 + 0.01 \times \mathrm{ECM} \times 365)/365 \times 100$ (Corré, 2002). Crosses indicate mean values, boxes represent interquartile ranges, and whiskers cover the full data range.

BGD
12, 3419–3468, 2015

Eddy covariance methane flux measurements over a grazed pasture

R. Felber et al.

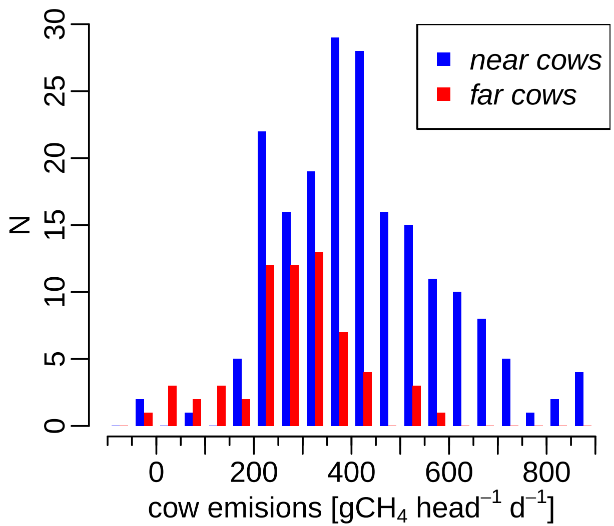

Figure 13. Histogram of cow emissions for *near cows* and *far cows* for the GPS method (according to Eqs. 3 and 4).

BGD
12, 3419–3468, 2015

Eddy covariance methane flux measurements over a grazed pasture

R. Felber et al.

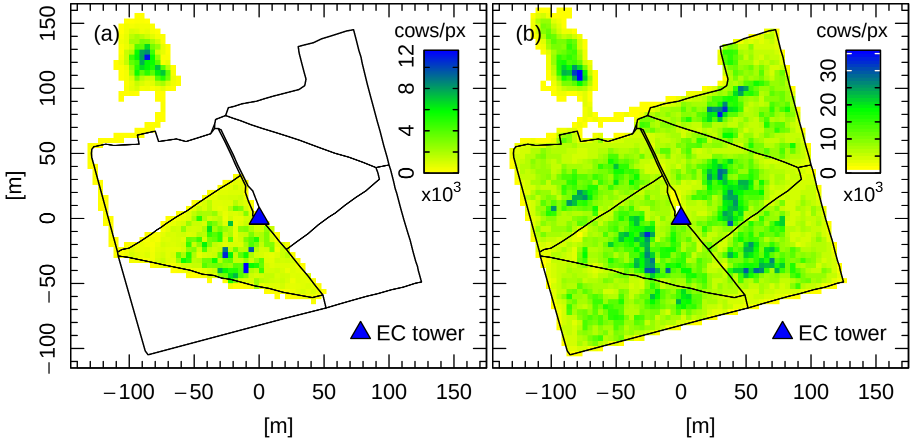

Figure 14. Cow density distribution **(a)** for one grazing cycle (i.e., two consecutive days) and **(b)** for the entire study field integrated over the full grazing season in 2013. The color of each pixel (4 m × 4 m) represents the number of data points collected at 5 s time resolution with the GPS trackers of all cows. Note the different color scales.